Phyllotactic Patterns on Plants

Patrick D. Shipman* and Alan C. Newell†

Department of Mathematics, University of Arizona, Tucson, Arizona 85721, USA

(Received 20 May 2003; published 23 April 2004)

We demonstrate how phyllotaxis (the arrangement of leaves on plants) and the deformation configurations seen on plant surfaces may be understood as the energy-minimizing buckling pattern of a compressed shell (the plant's tunica) on an elastic foundation. The key new idea is that the strain energy is minimized by configurations consisting of special triads of almost periodic deformations. We reproduce a wide spectrum of plant patterns, all with the divergence angles observed in nature, and show how the occurrences of Fibonacci-like sequences and the golden angle are natural consequences.

DOI: 10.1103/PhysRevLett.92.168102 PACS numbers: 87.15.La, 62.20.Dc, 87.10.+e

It has long been recognized that plant leaves, florets, and stickers are organized in patterns consisting of whorls or spirals which often obey Fibonacci rules [1]. Likewise, deformations of plant surfaces are observed to consist of quasiregular polyhedra, especially hexagonlike shapes [Fig. 1(a)] and ridges [Fig. 1(b)] [2]. How are such patterns produced? In [3], Douady and Couder introduced an ingenious magnetomechanical paradigm in which interacting magnetic dipoles reach an energy-minimizing configuration of whorls or spirals. Real plant surfaces, however, are not pools in which mutually interacting leaves float. The seminal works of Green and co-workers [4] and Dumais and Steele [5] have demonstrated through experiments that mechanical forces influence pattern choice and that there are correlations between the regions of compressive stress on a plant shoot and the regions where phyllotactic patterns are formed. In this Letter we show how minimizing the elastic energy of the plant surface postdicts spiral and whorl patterns, how transitions between patterns occur, and how patterns with hexagons and spirals [Fig. 1(a)] compete with ridges [Fig. 1(b)] and alternating 2-whorls [Fig. 1(c)].

Numbering the leaves on a plant (or stickers on a cactus, florets of a flower, etc.) according to their distance from the growth tip, one notes [see Fig. 1(a)] (i) that the angle between consecutively numbered leaves is constant for the plant, called the divergence angle, and (ii) that the distances from the growth tip of consecutive leaves are either of constant difference [as in Fig. 1(b)] or ratio [as in Fig. 1(a)], called the plastochrone difference or ratio. A consequence of these two observations is that the leaves form a lattice in the plane of the radial r (plastochrone difference) or $\ln(r)$ (plastochrone ratio) and circumferential angle α coordinates on the plant surface. One can choose minimal-length generators of the phyllotactic lattice of the form $\frac{1}{g}(m\lambda, 2\pi(md - q))$, $\frac{1}{g}(n\lambda, 2\pi(nd - p))$, where m, n, p, q, and g are integers such that $pm - nq = \gcd(m, n) = g$, and $2\pi d$ and λ are, respectively, the divergence angle and the plastochrone difference or ratio. The pair of integers (m, n) is called the parastichy pair. For plants that exhibit spirals [Figs. 1(a) and 1(b)], leaves lie at the intersection of m (n) spirals emanating clockwise (anticlockwise) from the growth tip. The pair (m, n) most often consists of consecutive members of the Fibonacci sequence [1], and the divergence angle is typically $2\pi d \simeq 2\pi\frac{p+q}{m+n}$.

Our picture is as follows [see Fig. 1(f)]: A region of active cell division and enlargement is located at the tip of a plant shoot. This region, called the shoot apical meristem (SAM), consists of a one- or two-cell-thick outer skin called the tunica (which we model as a spheroidal shell of thickness h with two local radii of curvature R_r and R_α in the radial and circumferential directions) connected to an inner squishy corpus of cells (which we model as an elastic foundation). Near the outer boundary of the SAM, the tunica hardens and experiences compressive stresses [5] due to a combination of growth pressures and the hardening process. As a consequence, the tunica buckles, forming bumps (primordia) on its surface that develop into new leaves or their analogs on, say, cacti or pine cones. New material emanating from the inner part of the SAM then becomes the material of the hardening apical region and it, in its turn, also buckles. Because the time scale for pattern formation is fast compared to the spreading, we model the hardening tunica region near the SAM boundary as an annular strip M of a thin spheroidal elastic shell lying over an elastic foundation a mean distance R from the north pole and treat all physical parameters as time independent. Our goal is to identify those buckling configurations which minimize the elastic energy. This initial model ignores influences of plastic or viscoelastic deformations; irreversibility is included by simply treating the elastic shell as being strongly overdamped.

The elastic energy $\mathfrak{E}$ is an integral over M with contributions from bending energy, strain energy, in-surface deformations, and an external potential containing the influences of the elastic foundation, radial pressure, and growth in the tunica (details will be given in an expanded version of this Letter). All of these can be written in

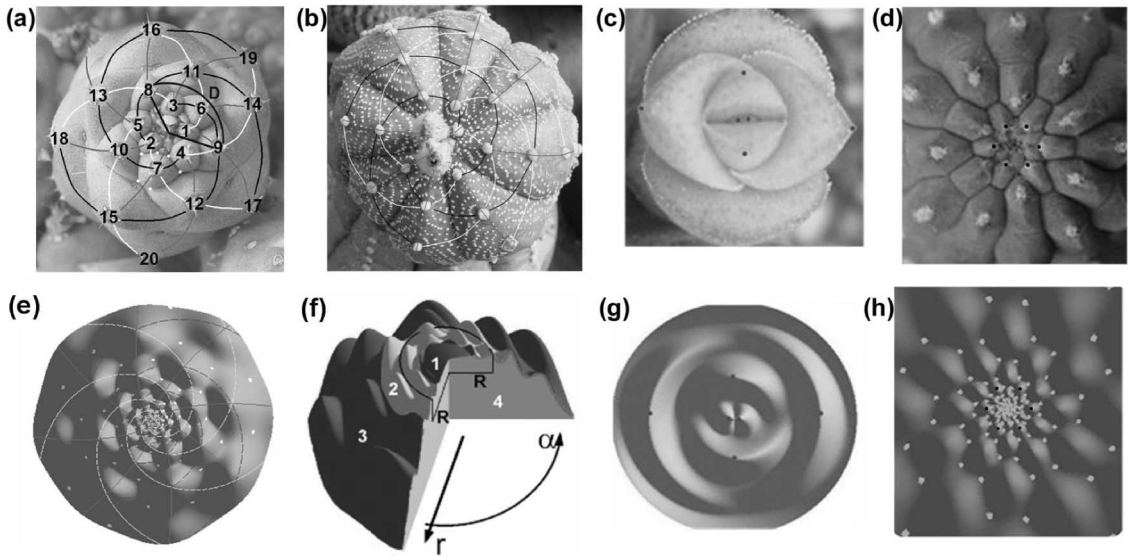

FIG. 1. (a) Cactus stickers are labeled according to their distance from the center. The divergence angle $D = 2\pi d$ is noted as are the families of 3,8 (5) spirals emanating clockwise (anticlockwise) from the center of the plant. Also note the irregular hexagons, one of whose vertices are marked in white. (b) This cactus also exhibits a 3,5-spiral arrangement, but the dominant pattern is the 8 (=3 + 5) radial ridges. (c) The maxima of the succulent surface are arranged in pairs that alternate in angle; this is the alternating 2-whorl (decussate) pattern. (d) Irregular hexagons are prominent on this cactus, whose stickers are arranged along 12 radial lines. (e) A theoretical reproduction of the cactus in (a). For the parameters $\Gamma = 4$, $\chi = 1$, $\frac{R_\alpha}{R_r} = 1$, the deformation consisting of three equal-amplitude states with the wave vectors k_4, k_5,k_6 of the standard phyllotactic wave vector sequence (SPWS) evaluated at $g = 1$ is an energy-minimizing configuration and is shown plotted on a sphere. The three families of spirals are also marked, as well as the vertices of irregular hexagons. (f) Schematic of a plant tip. The shoot apical meristem (SAM) consists of region 1 (undifferentiated tissue) and region 2 (the annular region M of average radius R where growth forces lead to buckling of the plant tunica). Tunica material goes from being in regions 1 to 2 to 3 as the shoot extends upward. Region 3 consists of material that has now hardened, thus setting the phyllotactic pattern developed when it was in region 2; the bumps may now develop into leaves, etc. Region 4 is the corpus of squishy material that acts as an elastic foundation to the tunica. (g) Theoretical reproduction of (c). In this energy-minimizing configuration found by minimizing the elastic energy with the parameters $\chi = 2$, $\Gamma = 1.7$ and restricted to the space consisting of the wave vectors $k_0 + k_2$,k_0,k_2,k_1 of the SPWS evaluated at $g = 2$, the first mode has an amplitude that is one-fifth the amplitude of the remaining modes. (h) Theoretical reproduction of cactus (d) found by restricting the energy, with $\chi = 2$, $\Gamma = 3$, to the space consisting of the wave vectors k_1,k_2,k_3 of the SPWS evaluated at $g = 6$. All modes have equal amplitude.

terms of the shell deformation $\omega(s, \alpha)$ normal to the original surface and the Airy stress function $F(s, \alpha)$, a potential for all surface stresses in the tunica. The radial variable s represents $r/\sqrt{R_\alpha h}$. In cases where growth is an increasing function of r, it is more appropriate to use a metric reflecting the fact that the shell is scale rather than Euclidean invariant. In that case s represents $\ln(r/\sqrt{R_\alpha h})$. Variations of $\mathfrak{E}$ with respect to ω and F give the von Kármán–Föppl–Donnell equations [6], $\zeta\omega_t = -\frac{\delta\mathfrak{E}}{\delta\omega}$ (a force equilibrium equation) and $\frac{\delta\mathfrak{E}}{\delta F} = 0$ (a compatibility equation), whose static solutions have the form $\omega_0 =$ const, $F_0 = -P(\chi s^2 + \alpha^2)$. The ratio of compressive stress in the angular direction ($\partial_s^2 F_0 = -P\chi$) to that in the radial direction ($\partial_\alpha^2 F_0 = -P$) is given by χ; results of [5] suggest that $\chi \geq 1$. The key parameters are the composite applied pressure P coming from growth in the corpus and the tunica and the aspect ratio $\Gamma = R/\sqrt{R_\alpha h}$, which measures the distance of the hardening region from the growth tip in units of the buckling wavelength and is the analog of G^{-1} in [3].

When the stress P is larger than some critical value P_c, the constant deformation state is linearly unstable and certain shapes and configurations are preferentially amplified. We write the deviation $w(s, \alpha, t)$ from ω_0 as $w = \sum_{j=1}^{N}[A_j(t)e^{il_j s + im_j \alpha} + \text{complex conjugate}]$ and the deviation $f(s, \alpha, t)$ from F_0 in terms of the complex amplitudes $A_j(t)$ by solving iteratively the compatibility equation $0 = \frac{\delta\mathfrak{E}}{\delta F}$. Substituting these expressions into $\mathfrak{E}$ and averaging over space, the perturbation energy $\mathfrak{E}(w, f)$ can be written in terms of the amplitudes A_j:

$$\mathfrak{E} = -\sum_{j=1}^{N} \sigma_j(l_j, m_j)A_j A_j^* - \sum \tau_{123}(A_1 A_2 A_3^* + A_1^* A_2^* A_3) + \sum_{c,d=1}^{N} \gamma_{cd} A_c A_c^* A_d A_d^*. \quad (1)$$

The *active* set A of $k_j = (l_j, m_j)$ is the set on which the (real) linear growth rates $\sigma(l_j, m_j)$ are greater than some small negative number (to allow for subcritical

bifurcations); also, the angular wave numbers m_j must be integers. The cubic terms in (1) arise from all triads of wave vectors $\mathrm{k}_1, \mathrm{k}_2, \mathrm{k}_3 = \mathrm{k}_1 + \mathrm{k}_2$ in A. The importance of such interactions leading to hexagonal planforms is well known from early works on convection and elasticity [7]. The coefficient τ_{123} arises from the strain energy and is a function of the triad wave vectors [8]. The quartic terms are positive definite and are mainly due to the elastic foundation (the squishy corpus). As the system is overdamped, the time dependence of the $A_j(t)$ are given by gradient flows $\zeta \frac{\partial}{\partial t} A_j = -\frac{\delta \mathfrak{E}}{\delta A_j^*}$, and therefore $\{A_j(t)\}_1^N$ relax to local minima in $\mathfrak{E}$. Our task is to find energy-minimizing configurations.

The key to success in this search (and the central message of this Letter) is the dominance of the triad interaction encoded by τ_{123}. Fibonacci-like sequences and hexagonal configurations occur precisely because of the dominance of triads, the former because the angular wave number of a triad follows Fibonacci addition rules induced by the condition $\mathrm{k}_1 + \mathrm{k}_2 = \mathrm{k}_3$. It is illuminating to write the wave vectors in a triad $\mathrm{k}_1 = (l_1, m_1)$, $\mathrm{k}_2 = (l_2, m_2)$, $\mathrm{k}_3 = (l_1 + l_2, m_1 + m_2)$ in terms of the phyllotactic coordinates introduced earlier as $l_1 = \frac{2\pi}{\lambda}(q - md)$, $m_1 = m$, $l_2 = \frac{2\pi}{\lambda}(p - nd)$, $m_2 = n$, where $pm - nq = \pm g = \pm \mathrm{gcd}(m, n)$. The intersection in the (s, α) plane of the lines $\mathrm{k}_j \cdot \mathrm{x} = 2\pi n_j$, $\mathrm{x} = (s, \alpha)$, $j = 1, 2, 3$, n_j an integer, are, for equal amplitudes A_j, the maxima of the deformation $w = \sum_{j=1}^{3} [A_j(t) e^{i l_j s + i m_j \alpha} +$ complex conjugate)] and occur on a lattice in the (s, α) plane generated by the phyllotactic lattice generators $\mathrm{v}_m = \frac{1}{g}(m\lambda, 2\pi(md - q))$, $\mathrm{v}_n = \frac{1}{g}(n\lambda, 2\pi(nd - p))$. The number λ is the dimensionless plastochrone difference or ratio depending on whether s represents $r/\sqrt{R_\alpha h}$ or $\ln(r/\sqrt{R_\alpha h})$. For $A_j = |A_j| e^{i\theta_j}$, and a given choice of m, n, $\tau_{123} = \tau(d, \lambda) \cos(\theta_1 + \theta_2 + \theta_3)$. It turns out that $\tau(d, \lambda)$ is, for large Γ, an extremely sensitive function of d and peaks dramatically at three special choices $\frac{q}{m}, \frac{p}{n}, \frac{p+q}{m+n}$ of d. Moreover, this Dirac delta function nature of $\tau(d, \lambda)$ is relatively insensitive to the physical parameters, except that some initial curvature in the region M (i.e., R_r, $R_\alpha < \infty$) is required; see below.

As the energy (1) is smaller when the coefficients σ_j and τ_{123} are larger, the simplest energy-minimizing configurations consist of the special triads of periodic deformations with local wave vectors $\mathrm{k}_1 = [\frac{2\pi}{\lambda}(q - md), m]$, $\mathrm{k}_2 = [\frac{2\pi}{\lambda}(p - nd), n]$, $\mathrm{k}_3 = [\frac{2\pi}{\lambda}(p + q - (m + n)d), m + n]$ in the set A and with $d \simeq \frac{q}{m}, \frac{p}{n}, \frac{p+q}{m+n}$. Because the linear growth rates are slightly larger for $d = \frac{p+q}{m+n}$, it turns out that the energy is minimized, quite independently of the physical parameters, at a value very close to $d = \frac{p+q}{m+n}$ and for $\theta_1 + \theta_2 + \theta_3 = 0$. The number λ is also chosen by energy minimization.

But we must also determine the choice of the integers m, n. To this end, first note that a plant begins its life with a smaller value of the radius R and therefore a smaller $\Gamma = R/\sqrt{R_\alpha h}$, but this parameter increases as the plant increases in size. For a fixed and moderate value of Γ, when the composite growth stress P exceeds P_c, the $\omega = \omega_0$ solution is unstable and the fastest growing modes are purely circumferential if $\chi > 1$. Among neighboring modes, the mode k_3, which also has a decomposition $\mathrm{k}_3 = \mathrm{k}_1 + \mathrm{k}_2$ where all three are in or close to the active set A, will, because τ_{123} is large, quickly destabilize again into an energy-minimizing configuration with three modes $\mathrm{k}_1 = [\frac{2\pi}{\lambda}(q - md), m]$, $\mathrm{k}_2 = [\frac{2\pi}{\lambda}(p - nd), n]$, $\mathrm{k}_3 = \mathrm{k}_1 + \mathrm{k}_2$, where d is approximately equal to $\frac{p+q}{m+n}$. This makes k_3 almost purely circumferential. As the plant slowly grows, Γ increases and the set of active modes (and therefore the energy-minimizing configuration) changes. Most often it is a neighboring triad of periodic deformations with wave vectors $\mathrm{k}_2, \mathrm{k}_3, \mathrm{k}_4 = \mathrm{k}_2 + \mathrm{k}_3$ which become the lowest energy configuration. A transition will occur and the plant will exhibit a combination of $\mathrm{k}_1, \mathrm{k}_2, \mathrm{k}_3$ and $\mathrm{k}_2, \mathrm{k}_3, \mathrm{k}_4$ configurations with the former (latter) more dominant in the outer (inner) region.

The standard phyllotactic wave vector sequence (SPWS) $k_0 = [\frac{2\pi}{\lambda}(-1), 0]$, $\mathrm{k}_1 = [\frac{2\pi}{\lambda}(1 - gd), g], \ldots$, where g is an integer and $\mathrm{k}_{j+2} = \mathrm{k}_j + \mathrm{k}_{j+1}$ encodes most of the configurations observed in nature (except those in which ridges, not triads dominate; see below). As Γ increases, the energy-minimizing triad moves upward in this sequence, with bifurcations (transitions) taking place between triads of modes with angular wave numbers $(0, g, g), (g, g, 2g), (g, 2g, 3g), \ldots, (m, n, m + n)$ and $d \simeq \frac{p+q}{m+n}$. For $g = 1$ (respectively, $g = 2$), the parastichy pair m, n consists of consecutive members of the Fibonacci sequence (respectively, the double Fibonacci sequence $2, 2, 4, \ldots$), and for $g = 1$, as m, n become large consecutive Fibonacci numbers, the divergence angle $2\pi \frac{p+q}{m+n}$ tends to the golden angle $2\pi[4/(1 + \sqrt{5})^2] \simeq 2\pi(0.381\,966)$ [9].

Figures 1(e) and 1(h) show examples of simple energy-minimizing configurations consisting of three periodic deformations. The steps taken to find the optimal configuration of Fig. 1(e) are as follows: For the choice of parameters stated in the caption, we compute the set A. For some values of d, the wave vectors $\mathrm{k}_4 = [\frac{2\pi}{\lambda}(1 - 3d), 3]$, $\mathrm{k}_5 = [\frac{2\pi}{\lambda}(2 - 5d), 5]$, $\mathrm{k}_6 = [\frac{2\pi}{\lambda}(3 - 8d), 8]$ of the SPWS evaluated at $g = 1$ all lie in A, and by computing the energy (1) for all these values of d, we find that it is the choice of $d \simeq 0.378 \simeq \frac{3}{8}$ that results in a minimization of the elastic energy $\mathfrak{E}$ restricted to the space spanned by the three wave vectors. Evaluating the elastic energy at $d = 0.378$, the stable stationary solution of the equations $\zeta \partial_t A_j = -\frac{\delta \mathfrak{E}}{\delta A_j^*}$, $j = 1, 2, 3$, is such that $|A_1| \simeq |A_2| \simeq |A_3| > 0$. Plotted in Fig. 1(e), then, is the deformation consisting of the triad of equal-amplitude periodic deformations of wave vectors $\mathrm{k}_4, \mathrm{k}_5, \mathrm{k}_6$ evaluated at $d = 0.378$. This results in a Fibonacci 3,5,8-spiral pattern. A similar

procedure produces the pattern illustrated in Fig. 1(h). Note, in particular, the (irregular) hexagons in Figs. 1(e) and 1(h).

This, however, is only part of the story. The choice of energy-minimizing amplitudes A_1, A_2, A_3 in a given triad may vary from the usual $|A_1| \simeq |A_2| \simeq |A_3|$ which produces the hexagonal configurations of Figs. 1(e) and 1(h) to a choice in which there is one clearly dominant amplitude $|A_1| \simeq |A_2| \ll |A_3|$, where k_3 is the almost purely circumferential mode with its ridges lying along radial lines. This occurs when τ_{123} is less dominant. The dominance of τ_{123} depends on the initial curvature of the plant near its growth tip. For less curved or flattish-topped plants (e.g., the saguaro) τ_{123} is small, and in this case it is the balance of the quadratic and quartic terms in (1) which is most important. For such plants, one usually does not observe Fibonacci-like sequences. There are also plants in which surface deformations are not best described by a single triad, but by a combination of two or more triads [see Fig. 1(g)]. These variations are included in our model but the results are left to a more detailed report which will also explicate the competition between ridges and hexagonal configurations and discuss defects in plant patterns.

P. D. S. was supported by NSF VIGRE Grant No. 9977116 and A. C. N. and P. D. S. were supported by NSF Grant No. DMS-0202440. We thank Michael Kücken for discussions.

*Email address: pship@math.arizona.edu
†Email address: anewell@math.arizona.edu

[1] R. Jean, *Phyllotaxis: A Systematic Study of Plant Morphogenesis* (Cambridge University, Cambridge, England, 1994).

[2] C. Innes and C. Glass, *Cacti* (Portland House, New York, 1991). Fine examples of hexagonal configurations are given by the species *Matucana krahnii* (p. 186) and *Tephrocactus geometricus* (p. 287).

[3] S. Douady and Y. Couder, Phys. Rev. Lett. **68**, 2098 (1992).

[4] P. Green, Int. J. Plant Sci. **153**, 59 (1992); P. Green, in *Dynamics of Cell and Tissue Motion*, edited by W. Alt *et al.* (Birkhäuser, Boston, 1997), pp. 243–249; P. Green, C. S. Steele, and S. C. Rennich, Ann. Bot. **77**, 515 (1996); C. S. Steele, J. Appl. Mech. **67**, 237 (2000).

[5] J. Dumais and C. S. Steele, J. Plant Growth Reg. **19**, 7 (2000); L. H. Hernández, A. Havelange, G. Bernier, and P. Green, Planta **185**, 139 (1991).

[6] P. Gould, *Plate and Shell Theory* (Prentice Hall, Englewood Cliffs, NJ, 1999).

[7] W. T. Koiter, Proc. K. Ned. Akad. Wet., B Phys. Sci. **66**, 265 (1963); F. H. Busse, Rep. Prog. Phys. **41**, 29 (1978).

[8] The coefficient τ_{123} arises from the strain energy triple product $f(w_{ss}w_{\alpha\alpha} - w_{s\alpha}^2)$. $\nabla^4 f$ is proportional to ω multiplied by the Gaussian curvature of the original surface. Therefore, for τ_{123} to play a role, the original surface must have curvature. Further, since the ratio of radial to circumferential derivatives in ∇^2 is of order Γ^2, f is maximized when one of these modes is almost circumferential.

[9] Denoting the kth Fibonacci number by f_k, prove by induction on j that $f_{j-1}f_j - f_{j-2}f_{j+1} = \pm 1$. The numbers $\frac{p+q}{m+n}$, then, can be chosen to be $(f_{j-1} + f_{j-2})/(f_j + f_{j+1}) = f_j/f_{j+2}$ (the other possible p, q choices yield similar results), and it is well known that f_j/f_{j+2} approaches the inverse of the golden number squared as j approaches infinity.